International Journal of Computer Information Systems and Industrial Management Applications.
ISSN 2150-7988 Volume 9 (2017) pp. 135-144

Representing ATS Drugs Molecular Structure Using 3D Orthogonal Fourier–Mellin Moments

Satrya Fajri Pratama[1], Noor Azilah Muda[1,✉], and Fadzilah Salim[2]

[1] Computational Intelligence and Technologies (CIT) Research Group,
Center of Advanced Computing and Technologies,
Faculty of Information and Communication Technology,
Universiti Teknikal Malaysia Melaka
Hang Tuah Jaya, 76100 Durian Tunggal, Melaka, Malaysia
satrya@student.utem.edu.my, azilah@utem.edu.my

[2] Department of Electrical Engineering Technology,
Faculty of Engineering Technology,
Universiti Teknikal Malaysia Melaka
Hang Tuah Jaya, 76100 Durian Tunggal, Melaka, Malaysia
fadzilah@utem.edu.my

***Abstract*: The campaign against drug abuse is fought by all countries, most notably on ATS drugs. The identification process of ATS drugs depends heavily on its molecular structure. However, the process becomes more unreliable due to the introduction of new, sophisticated, and increasingly complex ATS molecular structures. Therefore, distinctive features of ATS drug molecular structure need to be accurately obtained. This paper formulates a novel 3D orthogonal Fourier–Mellin moments-based molecular descriptor to represent the drug molecular structure. The performance of the proposed technique was analyzed using drug chemical structures obtained from UNODC for the ATS drugs, while non-ATS drugs are obtained randomly from ChemSpider database. The evaluation shows the proposed technique is qualified to be further explored and adapted in the future works to be fully compatible with ATS drug identification domain.**

***Keywords*:** 3D moments, ATS drugs, drugs identification, orthogonal Fourier–Mellin moments, molecular similarity, molecular descriptors**.**

I. Introduction

Amphetamine-type Stimulants (ATS) drug abuse, such as amphetamine, methamphetamine, and substances of the "ecstasy"-group, is recognized as universal, disturbing social delinquents. The struggles of finding tangible resolution of drugs abuse prevention are encountered by every national law enforcement authorities, because of the presence of new variety or unidentified ATS drugs. Nevertheless, the focus of cheminformatics research community is toward the advancement of chemical compounds that induces preferred biological outcome. Contrariwise, less devotion is demonstrated to the molecular similarity search which can be used to identify unfamiliar substances.

Ordinarily, the identification process depends on the chemical composition and conformation of a molecule, or generally referred as molecular structure. However, relying on these criteria alone for identification has been proved to be more undependable, mainly because the designs of novel ATS molecular structures are continuously more complex and sophisticated. Furthermore, it is a challenge for national law enforcement authorities and scientific staff of forensic laboratories, because present testing unit is very inadequate to identify new variety or unidentified ATS drug, in addition to likely detecting false negatives. Due to these limitations, it is preferable to perform the identification by relying on the shape of molecular structures.

The shape of molecular structures basically can be represented by using both of 2-dimensional (2D) and 3-dimensional (3D) model, which can be described numerically using shape descriptors. There are two types of 2D shape descriptors, which are boundary-based and area-based. On the other hand, 3D shape descriptors are emphasized into volume- and surface-based descriptors. It is commonly pronounced that 3D shape descriptor as more potent and more correctly represents an object's shape. Thus, this study believes that 3D descriptor is capable to identify distinctive features of ATS drug's molecular structure, notwithstanding new variety of ATS drug, because of its analogous ring substitutes.

This paper aims to propose a novel 3D Fourier–Mellin moments to represent the ATS drug molecular structure. The remainder of the paper is organized as follows. The ensuing section will provide a summary of ATS drug molecular structure similarity search, while an overview of existing 3D shape descriptors and 3D molecular descriptors is provided in Section 3. In Sections 4 and 5, the proposed technique is introduced and the experimental setup describing the data source collection and experimental design are presented respectively, while the results are discussed in Section 6. Finally, conclusion and future work is drawn in Section 7.

II. ATS Drug Molecular Structure Representation

United Nations Office of Drugs and Crime (UNODC) have outlined a set of standard methods to perform identification of ATS drugs to determine the exact, or at least similar, molecular structure. However, forensic laboratories staff occasionally doesn't meticulously follow these standards, hence the fluctuations of results attained from different testing laboratories is expected. However, most of testing laboratories agree that the most effective method for chemical substance identification is Gas Chromatography/Mass Spectrometry (GC/MS) [1]–[3].

Ref. [4] found that GC/MS is imperfect in identifying several varieties of ATS drugs, particularly methamphetamine. There are two stereo-isomers of methamphetamine, which are *l*-methamphetamine and *d*-methamphetamine. Ref. [5] terms isomers as "one of several species (or molecular entities) that have the same atomic composition (molecular formula) but different line formulae or different stereo-chemical formulae and hence different physical and/or chemical properties." Moreover, GC/MS is gradually more powerless in determining numerous substances with altered conformations are ATS drugs. Whereas *l*-methamphetamine gives meager pharmacodynamics effect, *d*-methamphetamine in contrast is a controlled substance which is frequently abused and severely addictive [6].

Drugs molecular structure heavily determines the results of manual identification process, which is continuously deteriorated with the introduction of new chemical compositions. Hence, false positive detection of ATS drugs is regularly occurred due to the flaws of present drug testing unit. Therefore, this study believes that by depending on the global shape of the molecular structure, the identification process can be refined. Molecular structures are often represented by 2D and 3D models. However, the characteristics of the ring substitutes in a molecule are imperceptible in 2D model, as opposed to 3D model. Hence, the latter is vital in discriminating the distinctive features at a ring substitute.

Geometrical shapes have been used for a long time to represent 2D and 3D molecular structures, and these geometric shapes can be describe numerically using shape descriptors. However, there is another type of molecular structure representation in the cheminformatics domain, which is known as molecular descriptors. Molecular descriptors are acquired after molecules are modeled into a molecular representation allowing for mathematical treatment [7]. Many researches are confronted by the difficulties in extracting the image or object shape features which can represent and describing the shape [8].

There are two types of molecular descriptors: topological or 2D descriptors and geometrical or 3D descriptors which derived from a geometrical representation. Since a geometrical representation comprises information of the relative positions of the atoms in 3D space, 3D descriptors generally offer supplementary information and more discrimination rule than 2D descriptors for same molecular structure. There are various 3D molecular descriptors exist, such as 3D-MoRSE descriptors, WHIM descriptors, GETAWAY descriptors, etc.

Invariance with respect to labelling, numbering of the molecule atoms, and molecule translation and rotation is a required property of a molecular descriptor. Furthermore, it also must have a clear algorithmically quantifiable definition, and the values must be in an appropriate numerical range for the molecule set where it is applicable to [9], [10]. Since a molecular descriptor is independent of the characteristics of the molecular representation, it is possible to consider the molecular shape as an image, and thus apply image processing to represent the shape of the molecular structure.

One of the applications of image processing methods to represent 2D and 3D image is Moment Invariants (MI), which can easily achieve these invariance properties. MI is a special case of Moments Function (MF). Moments are scalar quantities used to characterize a function and to capture its crucial features [11]. The first application of MI to represent molecular structure is 3D Zernike descriptors [12]. Although it was introduced to represent the molecular surface of protein structure, it provides an adequate motivation for further exploration of engaging MI as a numerical representation of molecule in the computer system, whether it is for molecular structure or for molecular surface.

There are several advantages of MI-based molecular shape representation compared to conventional representations. First, MI-based descriptors allow for fast retrieval and comparison of molecular structures. Second, due to its roto-translation invariance properties, molecular structures need not be aligned for comparison. Lastly, the resolution of the description of molecular structures can be easily and naturally adjusted by changing the order of shape descriptors [12], [13].

On the other hand, deriving MI from an MF technique is rather difficult, since it must satisfy the invariance requirements where an object representation must be invariant when said object is underwent translation, scale, and rotation transformation [14]. Therefore, this study only proposes a MF-based instead of MI-based molecular representation technique. This is because the development of MI-based molecular representation technique will be conducted extensively in the future works, and this study will be used as the basis of the MI-based technique, should this study exhibit satisfactory results.

Before the proposed technique is described and the justification of the results produced is presented, the existing MF-based techniques, which are going to be used as the comparison for the proposed technique, must be discussed first. These existing techniques will be presented the following section.

III. Existing Moments Techniques

Shape is an important visual feature and it is one of the basic features used to describe image content [15], and hence, searching for an image by using the shape features gives challenges for many researches, since extracting the features that represent and describe the shape is an arduous task [8]. In pattern recognition problem, there are many shape representations or description techniques have been explored to extract the features from the object, and one of the most commonly used is moments. A decent shape descriptor should be able to find perceptually similar shape where it usually means rotated, translated, scaled and affine-transformed

shapes. Furthermore, it can tolerate human beings in comparing the image shapes.

Moments can be used to generate a set of numbers that uniquely represent the global characteristic of an image, and has been used in diverse fields ranging from mechanics and statistics to pattern recognition and image understanding [16]. The use of moments to calculate image features in image analysis and pattern recognition was inspired by [17] and [18]. Moments are scalar quantities used to characterize a function and to capture its crucial features, or from the mathematical point of view, moments are projections of a function onto a polynomial basis.

A 2D image is considered as piece-wise continuous real function $f(x,y)$ of two variables defined on a compact support $D \subset R \times R$ and having a finite nonzero integral, which by extension is also applicable to 3D images. Moments of a 2D image $f(x,y)$ and 3D image $f(x,y,z)$ are usually denoted by

$$M_{pq} = \iint_D p_{pq}(x,y) f(x,y)\,\mathrm{d}x\,\mathrm{d}y \tag{1}$$

$$M_{pqr} = \iiint_D p_{pqr}(x,y,z) f(x,y,z)\,\mathrm{d}x\,\mathrm{d}y\,\mathrm{d}z \tag{2}$$

where p,q,r are non-negative integers, $s = p+q$ in case of 2D image or s $s = p+q+r$ in case of 3D image, is called the order of the moment, and $p_{pq}(x,y)$ or $p_{pqr}(x,y,z)$ are polynomial basis functions defined on D. Based on the polynomial basis $p_{pq}(x,y)$ or $p_{pqr}(x,y,z)$ used, there are various systems of MF can be recognized.

Additionally, if the polynomial basis $p_{pq}(x,y)$ is orthogonal, specifically if its elements satisfy the condition of (weighted) orthogonality

$$\iint_\Omega w(x,y) p_{pq}(x,y) p_{mn}(x,y)\,\mathrm{d}x\,\mathrm{d}y = 0 \tag{3}$$

for any indices $p \neq m$ or $q \neq n$ and Ω is the area of orthogonality, the MF are categorized as orthogonal moments function (OMF) [19]–[22]. The weight function $w(x,y)$ in some OMF, however, are not required. Some of the existing and well-known MF, including OMF, are discussed in the following sections.

A. Geometric Moments

The simplest choice of the polynomial basis is a standard power basis $p_{pq}(x,y) = x^p y^q$ leads to geometric moments, first introduced by [17], defined as

$$m_{pq} = \int_{-\infty}^{\infty}\int_{-\infty}^{\infty} x^p y^q f(x,y)\,\mathrm{d}x\,\mathrm{d}y \tag{4}$$

where $p,q = 0,1,2$ .... The formula can also be generalized to 3D geometric moments [23]

$$m_{pqr} = \int_{-\infty}^{\infty}\int_{-\infty}^{\infty}\int_{-\infty}^{\infty} x^p y^q z^r f(x,y,z)\,\mathrm{d}x\,\mathrm{d}y\,\mathrm{d}z \tag{5}$$

B. Complex Moments

Complex moments were originally proposed by [24] and later extended by [25] due to very little researches devoted to the independence of the invariants. The independence of the features is a fundamental issue in all the pattern recognition problems, especially in the case of a high-dimensional feature space. Complex moment c_{pq} of the order $p+q$ of an integrable image function $f(x,y)$ is defined as

$$c_{pq} = \int_{-\infty}^{\infty}\int_{-\infty}^{\infty} (x+y\hat{\imath})^p (x-y\hat{\imath})^q f(x,y)\,\mathrm{d}x\,\mathrm{d}y \tag{6}$$

where $p,q = 0,1,2$ ..., and $\hat{\imath}$ denotes the imaginary unit. Each complex moment can be expressed in terms of geometric moments m_{pq} as

$$\mu_{pq} = \sum_{\mathrm{i}=0}^{p}\sum_{j=0}^{q}\binom{p}{i}\binom{q}{j}(-1)^{q-j}\hat{\imath}^{p+q-i-j} m_{q-j,p+q-i-j} \tag{7}$$

In polar coordinates, (6) becomes

$$c_{pq} = \int_{-\infty}^{\infty}\int_{-\infty}^{\infty} r^{p+q+1} e^{\hat{\imath}(p-q)\varphi} f(r,\varphi)\,\mathrm{d}r\,\mathrm{d}\varphi \tag{8}$$

where $r = \sqrt{x^2+y^2}$ and $\varphi = \arctan\left(\frac{y}{x}\right)$ are the length of the vector from the origin to the pixel (x,y) and the angle between the vector r and the principle x-axis, respectively, with $r \in [-1,1]$ and $-\pi \leq \varphi \leq \pi$, and $c_{pq} = \overline{c_{qp}}$.

Recently, [26] proposed a 3D complex moments as the extension to 2D complex moments. The 3D complex moments can be defined as projections on the corresponding spherical harmonics times ϱ^s

$$\begin{aligned} c_{sl}^m &= \int_0^{2\pi}\int_0^{\pi}\int_0^{\infty} \varrho^{s+2} Y_l^m(\theta,\varphi)\sin\theta\, f(\varrho,\theta,\varphi)\,\mathrm{d}\varrho\,\mathrm{d}\theta\,\mathrm{d}\varphi \\ s &= 0,1,\ldots \\ l &= \begin{cases} 0,2,4,\ldots,s-2,s & s \text{ is even} \\ 1,3,5,\ldots,s-2,s & s \text{ is odd} \end{cases} \\ m &= -l,-l+1,\ldots,l \end{aligned} \tag{9}$$

where $\varrho = \sqrt{x^2+y^2+z^2}$, $\theta = \arctan\left(\frac{y}{x}\right)$, $\varphi = \arccos\left(\frac{z}{\varrho}\right)$, s is the order of the moment equals to $p+q$ in 2D, l is called latitudinal repetition equals to the index difference $p-q$ in 2D, m is a new index called longitudinal repetition, $\varrho^2 \sin\theta$ is the Jacobian of the transformation of Cartesian to spherical coordinates ϱ,θ,φ, and $Y_l^m(\theta,\varphi)$ is the spherical harmonics given as

$$Y_l^m(\theta,\varphi) = \sqrt{\frac{2l+1}{4\pi}\frac{(l-m)!}{(l+m)!}} P_l^m(\cos\theta)\, e^{\hat{\imath}\varphi} \tag{10}$$

where P_l^m is an associated Legendre function defined as

$$P_l^m(a) = (-1)^m (1-a^2)^{\frac{m}{2}} \left(\frac{\mathrm{d}}{\mathrm{d}a}\right)^m L_l(a) \tag{11}$$

and $L_l(a)$ is a Legendre polynomial defined as

$$L_s(a) = \sum_{k=0}^{s} c_{k,s} a^k = \frac{(-1)^s}{2^s s!} \left(\frac{\mathrm{d}}{\mathrm{d}a}\right)^s [(1-a^2)^s] \tag{12}$$

Since $Y_l^{-m} = (-1)^m \overline{Y_l^m}$, it can be derived that $c_{sl}^{-m} = (-1)^m \overline{c_{sl}^m}$.

C. Legendre Moments

Legendre moments were proposed by [27] because Legendre moments can be used to represent an image in Cartesian domain, with a near zero value of information redundancy [28]. Legendre moments of order $p+q$ is defined as [29]

$$\lambda_{pq} = \frac{(2p+1)(2q+1)}{4} \int_{-1}^{1}\int_{-1}^{1} L_P(x) L_q(y) f(x,y)\, \mathrm{d}x\, \mathrm{d}y \tag{13}$$

where $p, q = 0,1, \ldots$. The sth-order Legendre polynomials are defined in (12), which can also be written as

$$L_s(a) = \sum_{k=0}^{\frac{|s|}{2}} (-1)^k \frac{(2s-2k)!}{2^s k!\,(s-k)!\,(s-2k)!} a^{s-2k} \tag{14}$$

The recursive relation of Legendre polynomials, $L_s(a)$, is given as

$$L_s(a) = \frac{(2s-1)aL_{s-1}(a) - (s-1)L_{s-2}(a)}{s} \tag{15}$$

where $L_0(a) = 1$, $L_1(a) = a$ and $s > 1$.

The set of Legendre polynomials $L_s(a)$ forms a complete orthogonal basis set on the interval $[-1,1]$

$$L_s(a) = \frac{(2s-1)aL_{s-1}(a) - (s-1)L_{s-2}(a)}{s} \tag{16}$$

where δ_{pq} is the Kronecker delta.

3D Legendre moments was proposed by [30] as the extension of 2D Legendre moments, which was derived directly from Legendre polynomials. Like 2D Legendre, the values must be scaled in the region of $-1 \le x, y, z \le 1$. The equations of 3D Legendre moments are defined as

$$\lambda_{pqr} = \frac{(2p+1)(2q+1)(2r+1)}{8} \times \int_{-1}^{1}\int_{-1}^{1}\int_{-1}^{1} L_P(x) L_q(y) L_r(z) f(x,y,z)\, \mathrm{d}x\, \mathrm{d}y\, \mathrm{d}z \tag{17}$$

D. Zernike Moments

The set of orthogonal Zernike moments was first introduced for image analysis by [27]. Although it is computationally complex if compared to other moment functions such as geometric and Legendre moments, Zernike moments had been proven to be superior in terms of their feature representation capability, image reconstruction capability, and low noise sensitivity [31].

Besides that, the orthogonal property also enables the separation of the individual contributions of each order moment to the reconstruction process. The two-dimensional Zernike moments of order p with repetition q of an image intensity function $f(r,\varphi)$, are defined as

$$Z_{pq} = \frac{p+1}{\pi} \int_0^{2\pi}\int_0^{1} \overline{V_{pq}(r,\varphi)} f(r,\varphi) r\, \mathrm{d}r\, \mathrm{d}\varphi \tag{18}$$

The pth order Zernike polynomials are defined as

$$V_{pq}(r,\varphi) = R_{pq}(r) e^{\hat{\imath} q\varphi} \tag{19}$$

$$R_{pq}(r) = \sum_{k=0}^{\frac{p+q}{2}} (-1)^k \frac{(p-k)!}{k!\left(\frac{p+|q|}{2}-k\right)!\left(\frac{p-|q|}{2}-k\right)!} r^{p-2k} \tag{20}$$

where $p - |q|$ is even, $0 \le |q| \le p$, $p \ge 0$.

The set of Zernike polynomials, $V_{pq}(r,\varphi)$ forms a complete orthogonal set on the interval $[-1,1]$ as

$$\int_{-1}^{1}\int_{-\pi}^{\pi} V_{pq}(r,\varphi)\overline{V_{p'q'}(r,\varphi)} r\, \mathrm{d}r\, \mathrm{d}\varphi = \begin{cases} \frac{\pi}{p+1}\delta_{pp'}\delta_{qq'} & p = p', q = q' \\ 0 & \text{otherwise} \end{cases} \tag{21}$$

and its radial polynomials also satisfy the orthogonality relation as

$$\int_{-1}^{1} R_{pq}(r)\overline{R_{p'q}(r)} r\, \mathrm{d}r = \begin{cases} \frac{1}{2(p+1)}\delta_{pp'} & p = p' \\ 0 & \text{otherwise} \end{cases} \tag{22}$$

The Zernike moments was first extended to 3D by [32]. The 3D Zernike moments can be determined by using the complex conjugate of 3D Zernike polynomials defined as

$$\Omega_{nl}^m(R) = \int_0^1\int_0^{2\pi}\int_0^{\pi} \overline{Z_{nl}^m(R)} f(R) \varrho^2 \sin\theta\, \mathrm{d}\varrho\, \mathrm{d}\theta\, \mathrm{d}\varphi \tag{23}$$

The 3D unit-ball Zernike polynomials in spherical coordinates is defined as

$$Z_{nl}^m(R) = R_{nl}(\varrho) Y_l^m(\theta,\varphi) \tag{24}$$

where $0 \le l \le n$, $-l \le m \le l$, $n-l$ is an even non-negative integer number, and $R = (\varrho,\theta,\varphi)^T$ is the spherical coordinates. $R_{nl}(\varrho)$ is the real-valued radial functions, and $Y_l^m(\theta,\varphi)$ is the spherical harmonics given in (10). Spherical harmonics are orthonormal on the surface of the unit sphere per the relation

$$\int_0^{\pi}\int_0^{2\pi} Y_l^m(\theta,\varphi) Y_{l'}^{m'}(\theta,\varphi) \sin\theta\, \mathrm{d}\theta\, \mathrm{d}\varphi = \delta_{ll'}\delta^{mm'} \tag{25}$$

$R_{nl}(\varrho)$ are radial functions constructed by [32] to rewrite the Zernike polynomials defined in (20) in Cartesian coordinates as

$$Z_{nl}^m(X) = \sum_{v=0}^{k} q_{kl}^v \|X\|^{2v} e_l^m(X) \tag{26}$$

where $2k = n - l$, $0 \le v \le k$, and X denotes the vector $X = (x,y,z)^T$. Here, e_l^m are the harmonic polynomials defined as

$$\begin{aligned} e_l^m(X) &= \varrho^l Y_l^m(\theta,\varphi) \\ &= \varrho^l c_l^m \left(\frac{x\hat{\imath}-y}{2}\right)^m c^{l-m} \\ &\times \sum_{\mu=0}^{\left\lfloor\frac{l-m}{2}\right\rfloor} \binom{l}{\mu}\binom{l-\mu}{m+\mu}\left(-\frac{x^2+y^2}{4c^2}\right)^\mu \end{aligned} \tag{27}$$

where $c = x + y\hat{\imath}$ is the complex variable and c_l^m is normalization factors defined as

$$c_l^m = c_l^{-m} = \frac{\sqrt{(2l+1)(l+m)!\,(l-m)!}}{l!} \tag{28}$$

while the harmonic polynomials with negative values of m are defined as

$$e_l^{-m}(X) = (-1)^m \overline{e_l^m(X)} \tag{29}$$

The coefficients q_{kl}^v are later determined to guarantee the orthonormality of (26) within the unit ball as

$$q_{kl}^v = \frac{(-1)^k}{2^{2k}}\sqrt{\frac{2l+4k+3}{3}}\binom{2k}{k}(-1)^v \frac{\binom{k}{v}\binom{2(k+l+v)+1}{2k}}{\binom{k+l+v}{k}} \tag{30}$$

The orthogonality relation of 3D Zernike polynomials is defined as

$$\frac{3}{4\pi}\int_{\|X\|\le 1} Z_{nl}^m(X)\overline{Z_{n'l'}^{m'}(X)}\,\mathrm{d}X = \delta_{nn'}\delta_{ll'}\delta^{mm'} \tag{31}$$

IV. Proposed 3D Orthogonal Fourier–Mellin Moments

The Fourier–Mellin moments were firstly proposed by [33] which is defined in a polar coordinate system (r,φ). The Fourier–Mellin moments can be expressed as

$$M_{pq} = \int_0^{2\pi}\int_0^{\infty} r^p f(r,\varphi)\exp(-\hat{\imath}q\varphi)\,r\,\mathrm{d}r\,\mathrm{d}\varphi \tag{32}$$

where $f(r,\varphi)$ is an image function, and the circular harmonic order $m = 0, \pm1, \pm2, \dots$. The Mellin transform order p is complex valued.

Ref. [34] later proposed the orthogonal Fourier–Mellin moments. Defined in a polar coordinate system over the interior of the unit circle, the orthogonal Fourier–Mellin moments were introduced as the generalized Zernike moments and the orthogonalized complex moments. The authors showed that the performance of orthogonal Fourier–Mellin moments is superior to that of the Zernike moments in term of image reconstruction and signal-to-noise ratio.

The orthogonal Fourier–Mellin are defined in a polar coordinate system over the unit circle as

$$\Phi_{pq} = \frac{1}{2\pi\rho_p}\int_0^{2\pi}\int_0^{1} f(r,\varphi)Q_p(r)\exp(-\hat{\imath}q\varphi)\,r\,\mathrm{d}r\,\mathrm{d}\varphi \tag{33}$$

where the circular harmonic order $q = 0, \pm1, \pm2, ...$, and the $Q_s(r)$ is a radial polynomial in r of degree s. Ref. [34] obtained the polynomials $Q_s(r)$ by applying the Gram–Schmidt orthogonalization process to the sequence of natural powers of r over the $0 \le r \le 1$

$$1, r, r^2, \dots, r^s \tag{34}$$

and showed that the polynomials $Q_s(r)$ are equal to

$$Q_s(r) = \sum_{k=0}^{s} \alpha_{sk} r^k \tag{35}$$

$$\alpha_{sk} = (-1)^{s+k}\frac{(s+k+1)!}{(s-k)!\,k!\,(k+1)!} \tag{36}$$

Therefore, the normalization constant in (33) is

$$\rho_s = \frac{1}{2(s+1)} \tag{37}$$

Here α_{sk} are called coefficients of the sth polynomial with s starting from zero. Note that the radial polynomial $Q_p(r)$ and the harmonic polynomial $\exp(-\hat{\imath}q\varphi)$ have irrelevant variables r and φ, and parameters p and q.

An alternative method has been proposed by [35] to calculate the radial polynomial coefficients α_{sk} recursively

$$\begin{aligned} \alpha_{s0} &= (-1)^s(s+1) \\ \alpha_{sk} &= -\frac{(s+k+1)(s-k+1)}{k(k+1)}\alpha_{s(k-1)} \end{aligned} \tag{38}$$

Compared to the original definition expressed in (36), this formula is more computationally efficient. Other than employing the radial polynomial coefficients α_{sk} as stated in (35), the radial polynomial $Q_s(r)$ can be calculated recursively as well. Its recursive formula was proposed by [36] and [37] as

$$\begin{aligned} Q_0(r) &= 1 \\ Q_1(r) &= -2 + 3r \\ Q_s(r) &= \frac{(2r(4s^2-1) - 4s^2)Q_{s-1}(r) - (s-1)(2s+1)Q_{s-2}(r)}{(s+1)(2s-1)} \end{aligned} \tag{39}$$

Derived from (39) directly, the following properties of radial polynomial $Q_s(r)$ can be determined

$$\begin{aligned} Q_s(0) &= (-1)^s(s+1) \\ Q_s(1) &= \sum_{s=0}^{s}\alpha_{sk} = 1 \end{aligned} \tag{40}$$

Since the set of $Q_s(r)$ is orthogonal over the range $0 \le r \le 1$ and

$$\int_0^1 Q_p(r)Q_q(r)r\,\mathrm{d}r = \alpha_p\delta_{pq} \tag{41}$$

where δ_{pq} is the Kronecker delta, the basis functions $Q_p(r)\exp(-\hat{\imath}q\varphi)$ in (33) are orthogonal over the unit circle.

The orthogonal Fourier–Mellin moments can be expressed as linear combinations of Fourier–Mellin moments defined in (32)

$$\Phi_{pq} = \frac{p+1}{\pi}\sum_{i=0}^{p}\alpha_{pi}M_{iq} \tag{42}$$

The polynomials $Q_p(r)\exp(-\hat{\imath}q\varphi)$ can be expressed as complex polynomials in $(x+y\hat{\imath})$ and $(x-y\hat{\imath})$

$$Q_p(r)\exp(-\hat{\imath}q\varphi) = \sum_{i=0}^{p} \alpha_{pi}(x+y\hat{\imath})^u (x-y\hat{\imath})^v \tag{43}$$

where $u = \frac{i-q}{2}$ and $v = \frac{i+q}{2}$. Therefore, the orthogonal Fourier–Mellin moments are linear combinations of complex moments

$$\Phi_{pq} = \frac{p+1}{\pi} \sum_{i=0}^{p} \alpha_{pi} c_{uv} \tag{44}$$

where the complex moments c_{pq} are defined in (6). In general, the number of zeros of the radial polynomials corresponds to the capability of the polynomials to describe high frequency components of the image function $f(x,y)$.

Compared with Zernike moments, $Q_s(r) = 0$ has s real and distinct roots which are nearly uniformly distributed in the interior of the unit circle, therefore, it requires a lower order of orthogonal Fourier–Mellin moments for the description of an image function than that of Zernike moments [34]. The most important advantage is that the orthogonal Fourier–Mellin moments have nearly uniformly distributed zero points over the radial interval $0 \le r \le 1$, whereas the zero points of the Zernike moments are in the region of large radial distance from the origin. Hence the Zernike moments have difficulty in describing small images [38].

This study proposes the extension of Fourier–Mellin moments for 3D images. The proposed 3D Fourier–Mellin moments is adopting the generalization of *n*-dimensional moments on a sphere [19], [20], and defined as

$$\Phi_{nl}^{m} = \frac{1}{2\pi\rho_n} \int_0^{2\pi}\int_0^{\pi}\int_0^{1} Q_n(\varrho)\overline{\left(Y_l^m(\theta,\varphi)\right)} \times f(\varrho,\theta,\varphi)\varrho \, \mathrm{d}\varrho \, \mathrm{d}\theta \, \mathrm{d}\varphi \tag{45}$$

where $Q_s(\varrho)$, $Y_l^m(\theta,\varphi)$, and ρ_s are the radial polynomial, the spherical harmonics, and normalization constant given in (35), (10), and (37), respectively.

The 3D orthogonal Fourier–Mellin moments are implemented in discrete domain for digital images, and thus (45) becomes

$$\Phi_{nl}^{m} = \frac{1}{2\pi\rho_n} \sum_{\varrho=0}^{1}\sum_{\theta=0}^{\pi}\sum_{\varphi=0}^{2\pi} Q_n(\varrho)\overline{(Y_l^m(\theta,\varphi))} \times f(\varrho,\theta,\varphi)\varrho^2 \sin\theta \tag{46}$$

and can be implemented in Cartesian coordinates as

$$\Phi_{nl}^{m} = \frac{1}{2\pi\rho_n} \sum_{x=0}^{N-1}\sum_{y=0}^{N-1}\sum_{z=0}^{N-1} Q_n(x,y,z)\overline{(Y_l^m(x,y,z))} f(x,y,z) \tag{47}$$

since $\varrho^2 \sin\theta$ is the Jacobian of the transformation of Cartesian to spherical coordinates ϱ, θ, φ, and after the substituting $\sin\theta\, e^{\hat{\imath}\varphi} = \frac{x+y\hat{\imath}}{\varrho}$, and $\cos\theta = \frac{z}{\varrho}$. In the next section, the performance of the existing and proposed techniques on ATS and non-ATS dataset is revealed.

V. Experimental Setup

With the goal stated in the section above, an empirical comparative study must be designed and conducted extensively and rigorously. A detailed description of the experimental method is provided in this section.

A. Dataset Collection

This section describes the process of transforming molecular structure of ATS drug into 2D and 3D computational data representation. ATS dataset used in this research comes from [2], which contains 60 molecular structures which are commonly distributed for illegal use. On the other hand, 60 non-ATS drug molecular structures, which are randomly collected from [39], is used as benchmarking dataset.

These structures are drawn in 2D molecular structure format using MarvinSketch 15.11.9.0 [40]. After the 2D molecular structure is created, the structure will be cleaned and transformed to 3D molecular structure, also by using MarvinSketch. The structure will be then saved as MDL MOL file. The MDL MOL file must be then converted to Virtual Reality Markup Language (VRML) format, because VRML format is the input type required for generating voxel data of 3D molecular structure. To convert MOL file to VRML file, Jmol 14.4.0 [41] is required. VRML file will be then voxelized to voxel grid data with 512 voxel resolution using binvox 1.21 program [42]. An example of 2D and 3D molecular structure of ecstasy, one of the ATS drugs, and its voxelized molecular structure is shown in Figs. Figure **1**, Figure **2**, and Figure **3** respectively.

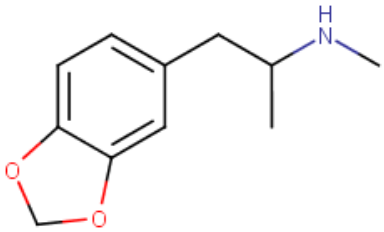

Figure 1. 2D molecular structure of ecstasy drawn using MarvinSketch [40]

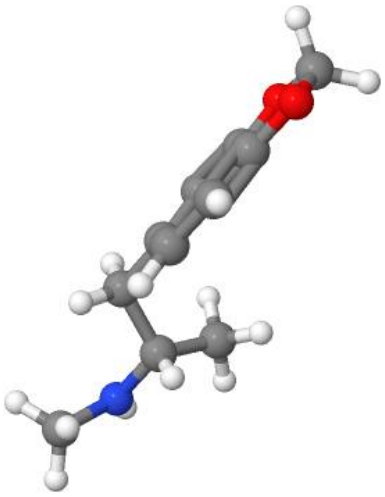

Figure 2. 3D molecular structure of ecstasy converted using Jmol [41]

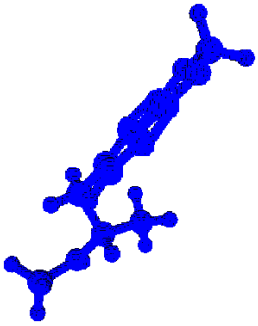

Figure 3. 3D molecular structure of ecstasy voxelized using binvox [42]

After the voxel data has been generated, 3D geometric, complex, Legendre, Zernike, and orthogonal Fourier–Mellin moments are calculated up to 8th order, which produces 165 features. While the features of 3D geometric and Legendre moments are real numbers, 3D complex, Zernike, and orthogonal Fourier–Mellin moments on the other hand are complex numbers.

Therefore, these complex numbers must be transformed into real numbers, because most of pattern recognition tasks only capable to handle real numbers. Ref. [43] proposed a method and four techniques to represent complex number as a real number, and they found Cartesian bit interleaved, one of the proposed technique, as the best representation technique. The value of the zeroth-order moments of ecstasy (3,4-methylenedioxy-methamphetamine), an example of ATS drug, for each 3D MF techniques represented using Cartesian bit interleaved are shown in Table 1. It should be noted that the molecular structure dataset for all formats (MDL MOL, VRML, and BINVOX), and computed and represented 3D moments are publicly available in [44].

B. Operational Procedure

The traditional framework of pattern recognition tasks, which are preprocessing, feature extraction, and classification, will be employed in this paper. This paper will compare the performance of existing and proposed 3D MF techniques. All extracted instances are tested using training and testing dataset discussed earlier for its processing time, memory consumption, intra- and inter-class variance, and classification of drug molecular structure using leave-one-out classification model, all of which are executed for 50 times.

Table 1. Cartesian bit interleaved values of zeroth-order moments of ecstasy for each 3D MF technique

MF	Original Number	Represented Number
Geometric	306425	42545721700200699567 041133799352041472
Complex	16130711836.2 18561	42576847550484374798 153183560267891362
Legendre	0.00028538051 9926548	14175173924443230618 113893434503725056
Zernike	7708.22998740 4831	42538108148786362155 157822007266511528
Fourier–Mellin	10277.6399832 06442	42538543586584499155 255924545490035232

To justify the quality of features from each MF technique in terms of intra- and inter-class variance, the quartile coefficient of dispersion (QCD) of normalized median absolute deviation (NMAD) is employed. The intra- and inter-class variance is a popular choice of measuring the similarity or dissimilarity of a representation technique [45]–[48]. The QCD measures dispersion and is used to make comparisons within and between data sets [49], and it is defined as

$$QCD_i = \frac{Q3_i - Q1_i}{Q3_i + Q1_i} \tag{48}$$

where $Q1_i$ and $Q3_i$ are the first and third quartile of the ith feature set, respectively. Meanwhile, the median absolute deviation (MAD) is a robust alternative to standard deviation as it is not affected the outliers [50], and it is defined as

$$MAD_i = \text{median}(|X_i - \text{median}(X_i)|) \tag{49}$$

where X_i is the set of error values for the ith feature. However, the MAD may be different across different instance, therefore it should be normalized to the original ith feature to achieve consistency for different data, such that

$$NMAD_i = \frac{MAD_i}{|x_i|} \times 100\% \tag{50}$$

In this study, the intra-class variance is defined as the QCD of NMAD for the i th feature of a molecular structure compared against intra-class molecular structures, and inter-class variance is defined as the QCD of NMAD for the ith feature compared against inter-class molecular structures.

On the other hand, the features are tested in terms of classification accuracy against well-known classifier, Random Forest (RF) [51] from WEKA Machine Learning package [52]. RF is employed in this study because previous studies conducted by [53]–[55] have found that RF is the most suitable for the molecular structure data. In this study, the number of trees employed by RF is 165, equals to the number of attributes of all 3D MF techniques.

VI. Experimental Results and Discussion

The existing and proposed MF techniques will be evaluated numerically in this section to evaluate their merit and quality in representing molecular structure. Table 2 presents the average of processing time, memory consumption, and the number of intra-class variance-inclined features relative to the total number of features, while Figure 4 present the average of classification accuracies from 50 executions.

Table 2. Processing time, memory consumption, and percentage of intra-class variance of 3D MF techniques

MF	Processing Time (ns/voxel)	Memory Consumption (bytes/voxel)	Intra-class Variance-inclined Features
Geometric	13	419	92.12%
Complex	39	841	77.58%
Legendre	16	1195	67.88%
Zernike	59	4405	64.24%
Fourier–Mellin	44	1923	62.42%

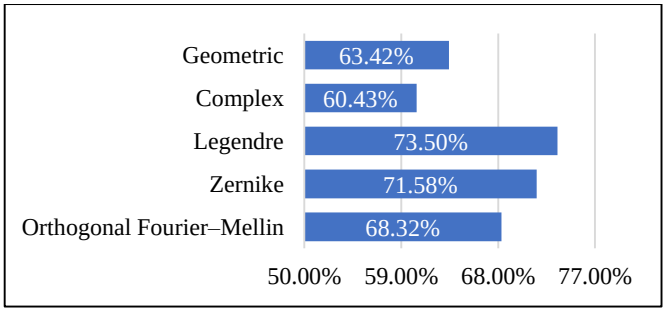

Figure 4. Average of classification accuracies of 3D MF techniques represented using Cartesian bit interleaved

The results presented in Table 2 show that 3D orthogonal Fourier–Mellin performs faster and requires less memory than Zernike moments. This is because the computation of radial polynomial of orthogonal Fourier–Mellin is less intricate than Zernike moments. However, 3D orthogonal Fourier–Mellin is slower than geometric and Legendre moments, but almost on par with complex moments, because the both complex and orthogonal Fourier–Mellin have the same complexity in computing the spherical harmonics. However, the number of intra-class variance-inclined features of 3D orthogonal Fourier–Mellin is the lowest among other 3D MF techniques.

On the other hand, the classification accuracy of 3D orthogonal Fourier–Mellin is higher than 3D geometric and complex moments, but not as high as 3D Legendre and Zernike moments. Since the classification accuracy is the primary consideration of this study, the classification accuracy should also be validated statistically. Prior to performing the statistical validation, the classification accuracy results should be tested for normality. If the results are normally distributed, ANOVA can be used to validate the classification accuracy, otherwise, Kruskal–Wallis H test should be used instead. In this study, the normality of the classification accuracy is tested using Shapiro–Wilk test of normality. The result of the test of normality is presented in Table 3.

The results in Table 3 shown that the classification accuracy for almost all 3D MF are normally distributed, since the p value of the Shapiro–Wilk test is greater the 0.05, except 3D geometric moments. The p value for this technique is below 0.05, and thus the data is significantly deviate from a normal distribution. Hence, Kruskal–Wallis H test must be selected instead to validate the random forests classification accuracy. After the Kruskal–Wallis H test is conducted, it is found that there is a statistically significant effect of the classification accuracy $[H(4) = 206.738, p = 0]$. Moreover, the ranks for the classification accuracy are shown in Table 4, with the post-hoc results using multiple Mann–Whitney U test statistic are shown in Table 5, comparing 3D orthogonal Fourier–Mellin moments against other 3D MF techniques.

Table 3. Tests of normality for classification accuracy of 3D MF techniques

MF	Statistic	*df*	Sig.
Geometric	0.933	50	0.007
Complex	0.978	50	0.48
Legendre	0.973	50	0.305
Zernike	0.975	50	0.353
Fourier–Mellin	0.981	50	0.596

Table 4. Ranks for the classification accuracy of 3D MF techniques

MF	*N*	Mean Rank
Geometric	50	71.69
Complex	50	33.47
Legendre	50	210.5
Zernike	50	179.56
Fourier–Mellin	50	132.28

Table 5. Post-hoc test results using multiple Mann–Whitney U tests for the classification accuracy of 3D orthogonal Fourier–Mellin against existing 3D MF techniques

Statistics	Geometric	Complex	Legendre	Zernike
Mann-Whitney U	186	10	123	412
Wilcoxon W	1461	1285	1398	1687
Z	-7.359	-8.563	-7.792	-5.802
Asymp. Sig. (2-tailed)	0	0	0	0
Bonferroni Threshold	0.005	0.005	0.005	0.005

Post-hoc comparisons using multiple Mann–Whitney U test on each pair of groups and adjusting the p value with the Bonferroni method, which is shown in Table 5, indicated that there is a statistically significant difference between the classification accuracy of 3D orthogonal Fourier–Mellin moments and other 3D MF techniques ($p = 0$). Therefore, it can be concluded that despite 3D orthogonal Fourier–Mellin moments cannot achieve the same level of classification accuracy of 3D Legendre and Zernike moments, it does indeed perform significantly better than 3D geometric and complex moments statistically.

Furthermore, the resource consumption of 3D orthogonal Fourier–Mellin is lower 3D Zernike moments, but not as low as other existing 3D MF techniques. However, 3D orthogonal Fourier–Mellin has the least number of intra-class variance-inclined features compared to other 3D MF techniques. Nevertheless, this study has proposed a new 3D MF technique and shown that the proposed 3D orthogonal Fourier–Mellin possesses certain potentials to be explored in the future, most notably on its invariance properties, despite its mediocre performance.

VII. Conclusion and Future Works

A new 3D MF technique to represent ATS drug molecular structure has been proposed and the extensive comparative study to the existing 3D MF techniques has been presented in this paper, namely 3D orthogonal Fourier–Mellin moments. Despite the experiments have shown that the proposed technique performs rather unexceptionally compared to existing 3D MF techniques in terms of processing time, memory consumption, intra- and inter-class variance, and more importantly, classification accuracy, this study nonetheless serves as a stepping stone towards better 3D molecular structure representation, especially on using continuous orthogonal moments defined on a sphere.

Hence, future works to extend the proposed technique so that it has invariance properties and to better represent the molecular structure based on this experimental study is required. The proposed feature extraction technique will be using specifically-tailored classifiers for drug shape representation, and ATS drug molecular structure data from National Poison Centre, Malaysia, will also be used as additional dataset in the future works.

Acknowledgment

This study is supported by UTeM Postgraduate Fellowship (Zamalah) Scheme from Universiti Teknikal Malaysia Melaka (UTeM), Malaysia and Collaborative Research Programme (CRP) – ICGEB Research Grant (CRP/MYS13-03) from International Centre for Genetic Engineering and Biotechnology (ICGEB), Italy.

References

[1] L.J. Langman, L.D. Bowers, J.A. Collins, C.A. Hammett-Stabler, M.A. LeBeau. "Gas Chromatography/Mass Spectrometry Confirmation of Drugs; Approved Guidelines - Second Edition". Pennsylvania, 2010.

[2] United Nations Office of Drugs and Crime. "Recommended Methods for the Identification and Analysis of Amphetamine, Methamphetamine and Their Ring-substituted Analogues in Seized Materials". *Sales No. E.06.XI.1*, New York, 2006.

[3] D.-L. Lin, R.-M. Yin, L.H. Ray. "Gas Chromatography-Mass Spectrometry (GC-MS) Analysis of Amphetamine, Methamphetamine, 3,4-Methylenedioxyamphetamine and 3,4-Methylenedioxymethamphetamine in Human Hair and Hair Sections", *Journal of Food and Drug Analysis*, 13(3), pp. 193-200, 2005.

[4] J.J. McShane. "GC-MS is Not Perfect: The Case Study of Methamphetamine". http://www.thetruthaboutforensicscience.com/gc-ms-is-not-perfect-the-case-study-of-methamphetamine/, 2011. Accessed 13 March 2012.

[5] International Union of Pure and Applied Chemistry. *Compendium of Chemical Terminology*, Blackwell Scientific Publications, Oxford, 2006.

[6] J. Mendelson, N. Uemura, D. Harris, R.P. Nath, E. Fernandez, P. Jacob, 3rd, E.T. Everhart, R.T. Jones. "Human pharmacology of the methamphetamine stereoisomers", *Clin Pharmacol Ther*, 80(4), pp. 403-420, 2006.

[7] R. Todeschini, V. Consonni. "Descriptors from Molecular Geometry", in *Handbook of Chemoinformatics*, Wiley-VCH Verlag GmbH, 2008.

[8] A.K. Muda. "Authorship Invarianceness for Writer Identification Using Invariant Discretization and Modified Immune Classifier". Universiti Teknologi Malaysia, 2009.

[9] V. Consonni, R. Todeschini. "Basic Requirements for Valid Molecular Descriptors". http://www.moleculardescriptors.eu/tutorials/T3_moleculardescriptors_requirements.pdf, 2006. Accessed 28 January 2016.

[10] M. Randić. "Molecular bonding profiles", *Journal of Mathematical Chemistry*, 19(3), pp. 375-392, 1996.

[11] Y. Sun, W. Liu, Y. Wang. "United Moment Invariants for Shape Discrimination". In: *International Conference on Robotics, Intelligent Systems and Signal Processing*, pp. 88-93, 2003.

[12] D. Kihara, L. Sael, R. Chikhi, J. Esquivel-Rodriguez. "Molecular Surface Representation Using 3D Zernike Descriptors for Protein Shape Comparison and Docking", *Current Protein and Peptide Science*, 12, pp. 520-530, 2011.

[13] L. Sael, B. Li, D. La, Y. Fang, K. Ramani, R. Rustamov, D. Kihara. "Fast protein tertiary structure retrieval based on global surface shape similarity", *Proteins*, 72(4), pp. 1259-1273, 2008.

[14] D. Xu, H. Li. "Geometric Moment Invariants", *Pattern Recognition*, 41(1), pp. 240-249, 2008.

[15] D. Zhang, G. Lu. "Shape-based Image Retrieval using Generic Fourier Descriptor", *Signal Processing: Image Communication*, 17(10), pp. 825-848, 2002.

[16] S.X. Liao. "Image Analysis by Moment". University of Manitoba, 1993.

[17] M.-K. Hu. "Visual pattern recognition by moment invariants", *IRE Transactions on Information Theory*, 8(2), pp. 179-187, 1962.

[18] F.L. Alt. "Digital Pattern Recognition by Moments", *Journal of the ACM*, pp. 240-258, 1962.

[19] J. Flusser, T. Suk, B. Zitová. *Moments and Moment Invariants in Pattern Recognition*, John Wiley and Sons, Ltd, West Sussex, 2009.

[20] J. Flusser, T. Suk, B. Zitová. *2D and 3D Image Analysis by Moments*, John Wiley and Sons, Ltd, West Sussex, 2016.

[21] S.X. Liao, M. Pawlak. "On image analysis by moments", *IEEE Transactions on Pattern Analysis and Machine Intelligence*, 18(3), pp. 254-266, 1996.

[22] M. Pawlak. *Image Analysis by Moments: Reconstruction and Computational Aspects*, Oficyna Wydawnicza Politechniki Wroclawskiej, Wroclaw, 2006.

[23] F.A. Sadjadi, E.L. Hall. "Three-dimensional moment invariants", *IEEE Trans Pattern Anal Mach Intell*, 2(2), pp. 127-136, 1980.

[24] Y.S. Abu-Mostafa, D. Psaltis. "Recognitive Aspects of Moment Invariants", *IEEE Transactions on Pattern Analysis and Machine Intelligence*, PAMI-6(6), pp. 698-706, 1984.

[25] J. Flusser. "On the Independence of Rotation Moment Invariants", *Pattern Recognition*, 33, pp. 1405-1410, 2000.

[26] T. Suk, J. Flusser, J. Boldyš. "3D rotation invariants by complex moments", *Pattern Recognition*, 48(11), pp. 3516-3526, 2015.

[27] M.R. Teague. "Image analysis via the general theory of moments*", *J. Opt. Soc. Am.*, 70(8), p. 920, 1980.

[28] C.H. Teh, R.T. Chin. "On image analysis by the methods of moments", *IEEE Transactions on Pattern Analysis and Machine Intelligence*, 10(4), pp. 496-513, 1988.

[29] R. Mukundan, K.R. Ramakrishnan. *Moment Functions in Image Analysis Theory and Application*, World Scientific Publishing Co. Pte. Ltd., Singapore, 1998.

[30] L.-Y. Ong, C.-W. Chong, R. Besar. "Scale Invariants of Three-Dimensional Legendre Moments". In: *Pattern Recognition, 2006. ICPR 2006. 18th International Conference on*, pp. 141-144, 2006.

[31] C.-Y. Wee, R. Paramesran. "On the computational aspects of Zernike moments", *Image and Vision Computing*, 25(6), pp. 967-980, 2007.
[32] N. Canterakis. "3D Zernike Moments and Zernike Affine Invariants for 3D Image Analysis and Recognition". In: *11th Scandinavian Conf. on Image Analysis*, pp. 85-93, 1999.
[33] Y. Sheng, J. Duvernoy. "Circular-Fourier–radial-Mellin transform descriptors for pattern recognition", *J. Opt. Soc. Am. A*, 3(6), pp. 885-888, 1986.
[34] Y. Sheng, L. Shen. "Orthogonal Fourier–Mellin moments for invariant pattern recognition", *J. Opt. Soc. Am. A*, 11(6), pp. 1748-1757, 1994.
[35] G.A. Papakostas, Y.S. Boutalis, D.A. Karras, B.G. Mertzios. "Fast numerically stable computation of orthogonal Fourier--Mellin moments", *IET Computer Vision*, 1(1), pp. 11-16, 2007.
[36] B. Fu, J.Z. Zhou, Y.H. Li, B. Peng, L.Y. Liu, J.Q. Wen. "Novel recursive and symmetric algorithm of fast computing two kinds of orthogonal radial moments", *The Imaging Science Journal*, 56(6), pp. 333-341, 2008.
[37] E. Walia, C. Singh, A. Goyal. "On the fast computation of orthogonal Fourier–Mellin moments with improved numerical stability", *Journal of Real-Time Image Processing*, 7(4), pp. 247-256, 2012.
[38] Z. Ping, R. Wu, Y. Sheng. "Image description with Chebyshev-Fourier moments", *J Opt Soc Am A Opt Image Sci Vis*, 19(9), pp. 1748-1754, 2002.
[39] Royal Society of Chemistry. "ChemSpider Database". http://www.chemspider.com, 2015.
[40] ChemAxon Ltd. "Marvin". http://www.chemaxon.com, 2016.
[41] Jmol. "Jmol: an open-source Java viewer for chemical structures in 3D". http://www.jmol.org/, 2016.
[42] P. Min. "binvox 3D mesh voxelizer". http://www.patrickmin/binvox, 2016.
[43] S.F. Pratama, A.K. Muda, Y.-H. Choo. "Arbitrarily Substantial Number Representation for Complex Number". In: *International Symposium on Research in Innovation and Sustainability*, 2017.
[44] Computational Intelligence and Technologies Research Lab. "Amphetamine-type Stimulants Drug Molecular Structure Dataset". http://ftmk.utem.edu.my/cit/downloads/ats-drugs, 2016.
[45] Z. He, X. Youb, Y.-Y. Tang. "Writer Identification Using Global Wavelet-based Features", *Neurocomputing*, 71(10–12), pp. 1831-1841, 2008.
[46] G. Leedham, S. Chachra. "Writer Identification Using Innovative Binarised Features of Handwritten Numerals". In: *Proceedings of 7th International Conference on Document Analysis and Recognition*, pp. 413-417, 2003.
[47] S.N. Srihari, S.-H. Cha, H. Arora, S. Lee. "Individuality of Handwriting: A Validation Study". In: *Sixth IAPR International Conference on Document Analysis and Recognition*, pp. 106-109, 2001.
[48] E.N. Zois, V. Anastassopoulos. "Morphological Waveform Coding for Writer Identification", *Pattern Recognition*, 33, pp. 385-398, 2000.
[49] D.G. Bonett. "Confidence interval for a coefficient of quartile variation", *Computational Statistics & Data Analysis*, 50(11), pp. 2953-2957, 2006.
[50] P.J. Rousseeuw, C. Croux. "Alternatives to the Median Absolute Deviation", *Journal of the American Statistical Association*, 88(424), pp. 1273-1283, 1993.
[51] L. Breiman. "Random Forests", *Machine Learning*, 45(1), pp. 5-32, 2001.
[52] M. Hall, E. Frank, G. Holmes, B. Pfahringer, P. Reutemann, I.H. Witten. "The WEKA Data Mining Software: An Update", *SIGKDD Explorations*, 11, pp. 10-18, 2009.
[53] S.F. Pratama, A.K. Muda, Y.-H. Choo, A. Abraham. "A Comparative Study of 2D UMI and 3D Zernike Shape Descriptor for ATS Drugs Identification", in *Pattern Analysis, Intelligent Security and the Internet of Things*, Abraham, A., Muda, A.K., Choo, Y.-H. (eds.), Springer International Publishing, 2015.
[54] S.F. Pratama, A.K. Muda, Y.-H. Choo, A. Abraham. "Exact Computation of 3D Geometric Moment Invariants for ATS Drugs Identification", in *Innovations in Bio-Inspired Computing and Applications*, Snášel, V., Abraham, A., Krömer, P., Pant, M., Muda, A.K. (eds.), Springer International Publishing, 2016.
[55] S.F. Pratama, A.K. Muda, Y.-H. Choo, A. Abraham. "3D Geometric Moment Invariants for ATS Drugs Identification: A More Precise Approximation", in *Proceedings of the 16th International Conference on Hybrid Intelligent Systems (HIS 2016)*, Abraham, A., Haqiq, A., Alimi, A.M., Mezzour, G., Rokbani, N., Muda, A.K. (eds.), Springer International Publishing, Cham, 2017.

Author Biographies

Satrya Fajri Pratama was born in Bandung, Indonesia on October 11, 1988. He received his Bachelor of Computer Science in Software Engineering and Master of Science in Information and Communication Technology from the Faculty of Information and Communication Technology, Universiti Teknikal Malaysia Melaka. He is currently pursuing his Doctor of Philosophy in Information and Communication Technology, also in Universiti Teknikal Malaysia Melaka. His research interests are including intelligent system, pattern recognition and software engineering.

Noor Azilah Muda is a Lecturer in Software Engineering Department, teaching theory and practical in software and database development related subjects. Noor Azilah's education was first in Bachelor Science in Agribusiness from University Putra Malaysia then Masters in Computer Science from Universiti Teknologi Malaysia. She was offered to join KUTKM as a lecturer in 2002 and since then she has been teaching various subjects and supervised many students. Noor Azilah's research interest is in the area of Soft Computing, Data Management and Software Engineering.

Fadzilah Salim received the BSc Mathematics from Purdue University, USA, and MA Further & Higher Education from Sheffield Hallam University, UK. She is currently with Universiti Teknikal Malaysia Melaka as a lecturer in Faculty of Engineering Technology. Her research interests are Mathematics and Math Education.